

EXPERIMENTAL STUDY OF MAGNETOSTATIC MODES  
IN A FERRITE SPHEROID

by

Christian F. Dreyer, Jr.

---

A Thesis Submitted to the Faculty of the  
DEPARTMENT OF ELECTRICAL ENGINEERING  
In Partial Fulfillment for the Requirements  
For the Degree of  
MASTER OF SCIENCE  
In the Graduate College  
THE UNIVERSITY OF ARIZONA

1 9 6 3

STATEMENT BY AUTHOR

This thesis has been submitted in partial fulfillment of requirements for an advanced degree at The University of Arizona and is deposited in The University Library to be made available to borrowers under rules of the Library.

Brief quotations from this thesis are allowable without special permission, provided that accurate acknowledgment of source is made. Requests for permission for extended quotation from or reproduction of this manuscript in whole or in part may be granted by the head of the major department or the Dean of the Graduate College when in their judgment the proposed use of the material is in the interests of scholarship. In all other instances, however, permission must be obtained from the author.

SIGNED: Christian F. Dreyer, Jr.

APPROVAL BY THESIS DIRECTOR

This thesis has been approved on the date shown below:

D. C. Stinson June 6, 1963  
D. C. Stinson Date  
Professor of Electrical Engineering

## ACKNOWLEDGMENT

The author wishes to acknowledge the assistance and guidance proffered by Dr. Donald C. Stinson without which this thesis would not have been possible. Sincere appreciation is also extended to the author's wife for her moral and material support during the preparation of this thesis.

## TABLE OF CONTENTS

	Page
LIST OF ILLUSTRATIONS . . . . .	v
ABSTRACT . . . . .	vi
 Chapter	
I    INTRODUCTION . . . . .	1
1.1    General Background . . . . .	1
1.2    Statement of the Problem . . . . .	2
1.3    Method of Attack . . . . .	3
II   THEORY . . . . .	5
2.1    Characteristics of the YIG . . . . .	5
2.2    Spin Wave Theory . . . . .	5
2.3    Magnetostatic Mode Theory . . . . .	8
2.4    Theory of the Cross Guide Coupler . . . . .	14
III  EXPERIMENTAL . . . . .	18
3.1    Experimental Arrangement . . . . .	18
3.2    Sample Configuration and Mounting . . . . .	20
3.3    Measurement Procedure . . . . .	23
3.4    Characteristic Assumptions for the Sample . . . . .	23
3.5    Experimental Results . . . . .	25
IV  CONCLUSIONS . . . . .	36
4.1    Conclusions . . . . .	36
4.2    Recommendations for Further Study . . . . .	37
REFERENCES . . . . .	38

## LIST OF ILLUSTRATIONS

Figure	Page
2.1 Precession of Spin Dipoles . . . . .	7
2.2 Suhl Dispersion Relation . . . . .	9
2.3 Plot of $(\omega/\gamma - H_1)/4\pi M_0$ Versus $H_0/4\pi M_0$ for Some of the Low Order Walker Modes . . . . .	13
2.4 Cross Guide Coupler Test Section . . . . .	16
3.1 Block Diagram of Component Arrangement . . . . .	19
3.2 Cross Section of the Cross Guide Coupler Showing the Locations of Ferrite Positions 1, 2, and 3 in the Aperture . . . . .	22
3.3 Coupled Power Versus H Applied for the Unpolished Ferrite . . . . .	26
3.4 Coupled Power Versus H Applied for the Polished Ferrite . . . . .	27
3.5 Plot of $\omega/\gamma 4\pi M = 0.842$ on Figure 2.3 . . . . .	29
3.6 Magnetostatic Modes in a Single Crystal YIG . . . . .	31
3.7 Line Width as a Function of Frequency for Sample in Position 1 . . . . .	32
3.8 Line Width as a Function of Frequency for Sample in Position 2 . . . . .	33
3.9 Line Width as a Function of Frequency for Sample in Position 3 . . . . .	34

## ABSTRACT

Ferrimagnetic resonance experiments were performed on a single crystal yttrium iron garnet at microwave frequencies ranging from 0.9 gc to 4.5 gc. Theoretical and experimental results showed that magnetostatic modes could be detected and identified employing the cross guide coupler technique. The number of modes excited, using the cross guide coupler technique, decrease as the surface finish is improved. Measurements of the line widths of the magnetostatic modes indicate that they are essentially the same at any one frequency.

## CHAPTER I

### INTRODUCTION

#### 1.1 General Background

The microwave applications of ferrites did not become important until the end of World War II. With the suggestion by Snoek<sup>1</sup> of the possibility of experimentally observing ferromagnetic resonance in ferrites at microwave frequencies, intensive studies were renewed. Subsequent observation of this resonance phenomena stimulated the search for new and improved materials. The ensuing research into the electromagnetic properties of ferrites led to the discovery of the rare earth garnets<sup>2,3</sup> and the growth of single crystal garnets.<sup>4</sup>

The single crystal garnets have the general formula  $M_3Fe_2(FeO_4)_3$  where M is the trivalent diamagnetic yttrium or any of the trivalent paramagnetic rare earth elements. Because of the unique crystal structure and the quality control obtainable in production, the yttrium iron garnet (hereafter designated YIG) has proved to be the most valuable for both basic research and high frequency applications. For these reasons the single crystal YIG will be used throughout this experiment.

About the same time as the discovery of the ferrite garnets, White, Solt, and Mercereau<sup>5,6</sup> and Dillon<sup>7</sup> observed a spectrum of multiple resonance absorption phenomena in ferrites. The general theory of these magnetostatic modes has since been formulated by Walker<sup>8</sup> wherein he also advanced a criterion for their identification which is not unlike the mode classification scheme used for waveguides and cavities. With minor corrections for propagation, which Walker neglected, experimental verification of his theory for a large number of modes was conducted by Fletcher, Solt and Bell<sup>9</sup> and an excellent comparison between calculated and observed values was obtained.

## 1.2 Statement of the Problem

Most of the experimental studies of magnetostatic modes reported in the literature have been performed in resonant cavities. Although extremely accurate, cavities are inherently difficult to instrument, not easily tunable over a large range of frequencies, and require a high degree of operator knowledge. These disadvantages have been overcome by the use of the cross guide coupler introduced by Stinson<sup>10</sup> for the measurement of ferrite line widths. This system has proved highly accurate in line width measurements and in the course of these experiments<sup>11</sup> magnetostatic modes have been observed, but no further

attempts have been made to study them. Therefore, it will be the purpose of this thesis to determine the practicality of using the cross guide coupler in exciting and identifying magnetostatic modes in a single crystal YIG. An earlier experiment<sup>11</sup> on line widths using the cross guide coupler technique reported a number of these modes between 2 and 4 gc. Therefore this experiment will include these frequencies.

Excitation of the different modes is dependent upon the symmetry of the rf magnetic field within the ferrite. In order to take advantage of all possible variations of the rf magnetization within the ferrite sphere it will be placed in several different positions within the coupling aperture of the cross guide coupler.

### 1.3 Method of Attack

Experiments will be performed at a number of rf frequencies between 0.9 and 4.5 gc on a ferrite sphere placed at three different locations in the cross guide coupler aperture. At each separate rf frequency the magnetostatic field will be varied throughout its range and the coupled power plotted as a function of the applied magnetostatic field. Sufficient points will be plotted so that an accurate determination of the line widths of multiple resonances can be obtained.

The YIG sphere will then be polished with 3/0 abrasive paper (15 micron grit size) and the experiments just described will be repeated to determine the effect of surface polish in exciting magnetostatic modes.

## CHAPTER II

### THEORY

#### 2.1 Characteristics of the YIG

In general the ferrites having a garnet crystal structure are superior to those of spinel or inverted spinel structure and this is particularly true of the yttrium iron garnet. The crystal structure of garnets is very nearly cubic and contains little or no magnetic irregularities.

The YIG is characterized by its small saturation magnetization and small magnetic anisotropy field when these values are compared with those normally observed in ferrites. High purity single crystal YIGs have very narrow line widths and their magnetic properties are much more reproducible than those of spinel structure. Therefore, they are ideally suited to a correlation between theory and experiment.

#### 2.2 Spin Wave Theory

At this point a qualitative discussion of spin waves will give us some insight into the process of energy losses in ferrites. Within a ferrite is a restoring force that tends to make all spin dipoles behave alike. If the

ferrite medium is saturated with a uniform magnetostatic field this tendency to behave alike is satisfied and the spin dipoles precess in phase with equal magnitude as shown in Fig. 2.1a.<sup>12</sup> A uniform rf field directed perpendicularly to the magnetostatic field will interact with the spin dipoles and cause them to precess in amplitude (increase the precession angle) and/or phase. Two easily depicted waves are shown as the standing wave (Fig. 2.1b) in which the amplitude varies but the phase is constant and the directed wave (Fig. 2.1c) in which the amplitude is constant and the phase varies.<sup>13</sup> The wave length is measured between two successive in-phase spins.

The classical equation of motion, neglecting damping, may be modified by the addition of a spin wave term

$$\frac{d\bar{M}}{dt} = \gamma(\bar{M} \times \bar{H}) + \gamma H_{ex} a^2 \frac{\bar{M} \times \nabla^2 \bar{M}}{\bar{M}} \quad (2-1)$$

where  $\gamma$  is the gyromagnetic ratio,  $H_{ex}$  is the exchange field, "a" is the lattice spacing and the vector quantity is the restoring term tending to align dipoles. Gaussian units are used throughout. Solution of the above equation for the resonant frequencies in terms of the spin wave number "k" is given by

$$\omega_k = (\omega_0 - N_z \omega_M + \omega_{ex} a^2 k^2)(\omega_0 - N_z \omega_M + \omega_{ex} a^2 k^2 + \omega_M \sin^2 \theta_k)^{1/2}$$

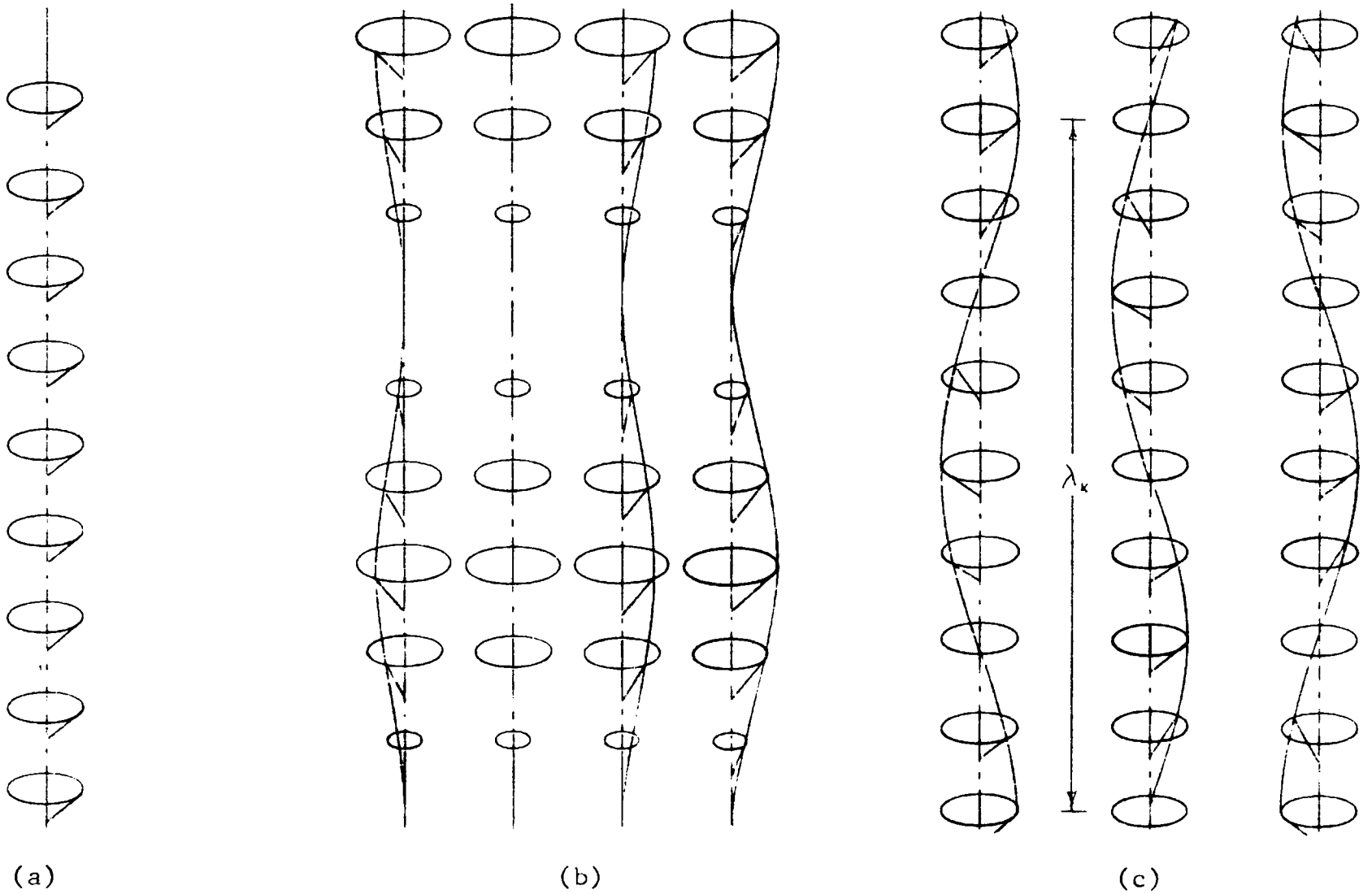


Figure 2.1.--Precession of Spin Dipoles. (a) In phase constant amplitude; (b) in phase different amplitude, (c) out of phase, constant amplitude. (After B. Lax and K. J. Button, McGraw-Hill Book Co., pp. 173-174, 1962).

where  $\omega_0 = \gamma H_0$ ,  $N_z$  is the demagnetizing factor in the direction of the applied magnetostatic field,  $\omega_M = \gamma 4\pi M_0$ , and  $\theta_k$  is the angle between the spin wave propagation and the magnetostatic field. A plot of the Suhl dispersion relation,<sup>14</sup> Figure 2.2, shows the relation of both spin waves and Walker modes to the wave number "k" for a spheroid. The frequency of the Kittel or uniform mode is given by the middle formula on the ordinate axis. Derivation of equation (2-2) assumed the existence of a medium much larger than the wave length of the spin wave. The plane wave analysis is generally considered acceptable for mediums at least ten times as large as the wavelength. For samples smaller than this value, the boundary problem must be solved. This is the Walker mode region.

### 2.3 Magnetostatic Mode Theory

The analysis of Walker's theory<sup>8</sup> begins with the equation of motion neglecting damping and exchange. This is

$$\frac{d\bar{M}}{dt} = \gamma(\bar{M} \times \bar{H}) \quad (2-3)$$

The ferrite sample is assumed to be a spheroid placed in a magnetostatic field and oriented such that magnetostatic field is along its easy magnetization direction, and both are z directed. The rf components will be signified by lower case letters and the static

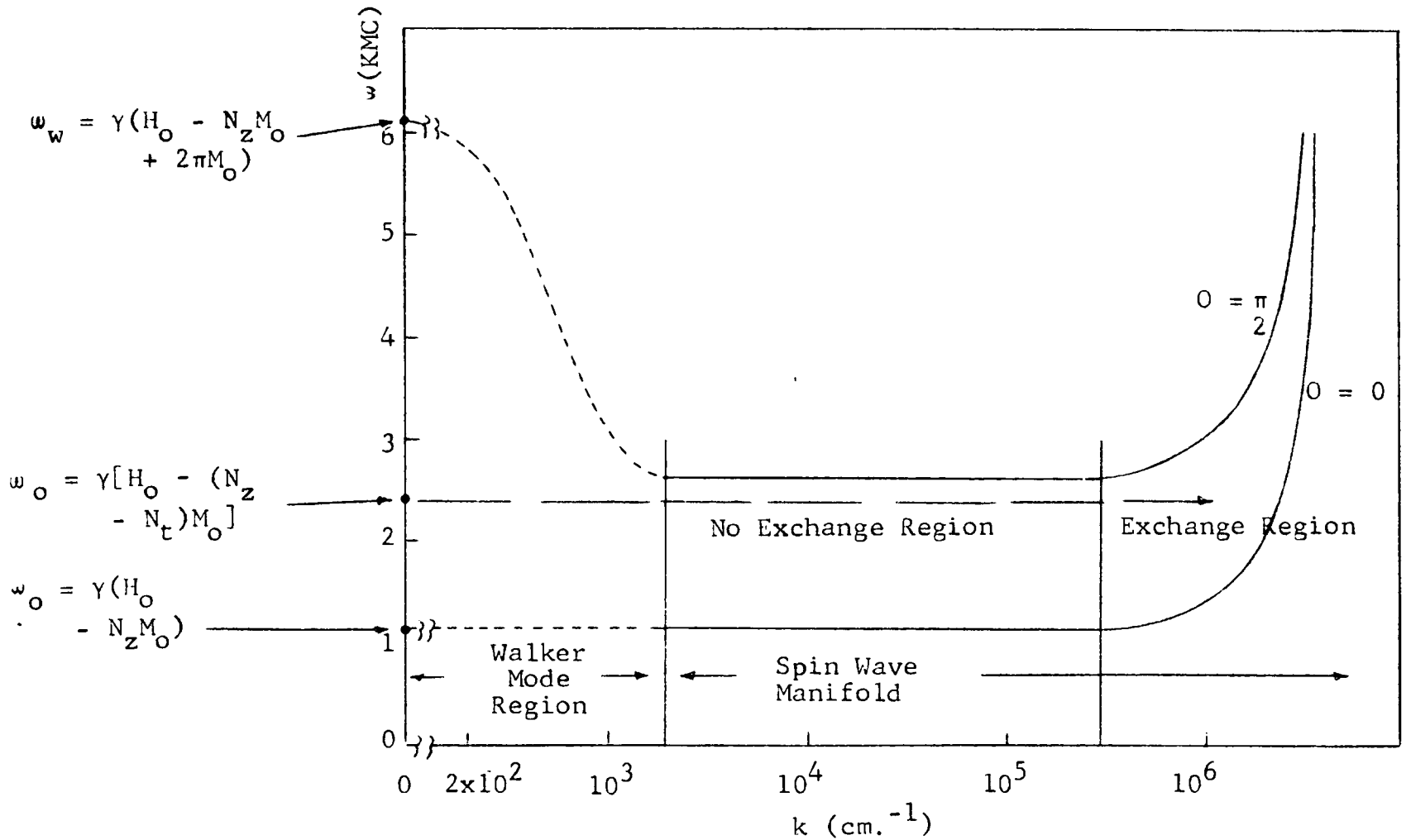


Figure 2.2.--Suhl Dispersion Relation (After C. R. Buffler, Gordon McKay Lab. of Appl. Science, S. R. No. 3, Ser. 2, February, 1960).

components by upper case. The internal static field  $H_i$  in a spheroid is  $H_o - 4\pi M_o N_z$ . The magnetization and magnetic fields are

$$\bar{M} = M_o \bar{a}_z + \bar{m} e^{j\omega t} \quad (2-4)$$

$$\bar{H} = H_i \bar{a}_z + \bar{h} e^{j\omega t}$$

For  $|\bar{m}| \ll |\bar{M}|$  and  $|\bar{h}| \ll |\bar{H}|$  Equation (2-3) becomes

$$j\omega m_x = \gamma (H_i m_y - M_o h_y) \quad (2-5)$$

$$j\omega m_y = \gamma (M_o h_x - H_i m_x)$$

Solutions for the rf magnetizations in terms of the susceptibility are

$$4\pi m_x = \chi_{xx} h_x - \chi_{yx} h_y \quad (2-6)$$

$$4\pi m_y = \chi_{yx} h_x + \chi_{xx} h_y$$

Under the assumption that we may ignore propagation, that is  $\text{div } \bar{b} = 0$ , the rf magnetization and magnetic field must satisfy  $\text{div } \bar{h} + \text{div } 4\pi \bar{m} = 0$  and  $\text{curl } \bar{h} = 0$ . The latter implies that we may introduce a scalar magnetic potential satisfying the equation  $\bar{h} = \text{grad } \psi$ . The divergence equation above then becomes

$$\nabla^2 \psi + \text{div } 4\pi \bar{m} = 0 \quad (2-7)$$

Substituting Equation (2-6) into (2-7) the wave equation within the sphere is

$$(1 + \chi_{xx}) \left( \frac{d^2}{dx^2} + \frac{d^2}{dy^2} \right) \psi + \frac{d^2}{dz^2} \psi = 0 \quad (2-8)$$

and outside the sphere

$$\nabla^2 \psi = 0 \quad (2-9)$$

The solution of Equation (2-9) in oblate spheroidal coordinates is of the form

$$\psi = Q_n^m(j\varepsilon) P_n^m(\delta) e^{jm\phi} \quad (2-10)$$

where the  $P_n^m$  and  $Q_n^m$  are Legendre functions of the first and second kind respectively, and the  $n$  and  $m$  are the mode indices. Solutions of (2-8) will be comprised of similar functions so that continuity of the tangential rf magnetic field and the normal component of  $\bar{b}$  is satisfied at the surface of the spheroid. The resultant equation is quite involved but a few of the pertinent facts will be brought forth. The transcendental equation has  $1 + 1/2[n - |m|]$  roots where  $[n - |m|]$  is the largest integer in  $n - |m|$ . Walker introduces a third index letter "r" where  $r + 1$  is the order of the root, thus the magnetostatic modes are identified by a three index  $(n, m, r)$  mode scheme.<sup>15</sup>

For the special case  $n$  equal to  $m$  or  $m + 1$  with  $r$  equal to zero the resonance expression for the modes is

$$\frac{\omega/\gamma - H_i}{4\pi M_0} = \frac{|m|}{G_{nm}(\alpha)} \quad (2-11)$$

where  $G$  is a ratio of Legendre polynomials as a function of the axial ratio of the spheroid. For the case of a perfect sphere  $G_{nm}(\alpha)$  reduces to  $n + 1 + m + (0, 1)$  taking 0 or 1 as  $n - |m|$  is even or odd respectively. Equation (2-1) then reduces to the simple form

$$\begin{aligned} \frac{\omega/\gamma - H_i}{4\pi M_0} &= \frac{m}{2m + 1} && \text{for } n = m \\ &= \frac{m}{2m + 3} && \text{for } n = m + 1 \end{aligned} \quad (2-12)$$

It is clear that the modes  $(m, m, 0)$  and  $(3m + 1, 3m, 0)$  are degenerate. A plot of  $(\omega/\gamma - H_i)/(4\pi M_0)$  versus  $H_0/4\pi M_0$  for some of the simple modes in the spherical case<sup>9</sup> is shown in Figure 2.3. The solutions of Equation (2-11) as a function of the axial ratio ( $\alpha$ ) for the simple modes indicate that this plot is sufficiently accurate for samples varying as much as five percent from a perfect sphere.

The mode structure is now complete when the basic assumption that there is no propagation is satisfied. Fletcher, Solt, and Bell<sup>9</sup> have shown that in general this assumption is not valid, although in the case of a single crystal YIG the error is only about one percent. The effects of propagation are twofold. First, there is a

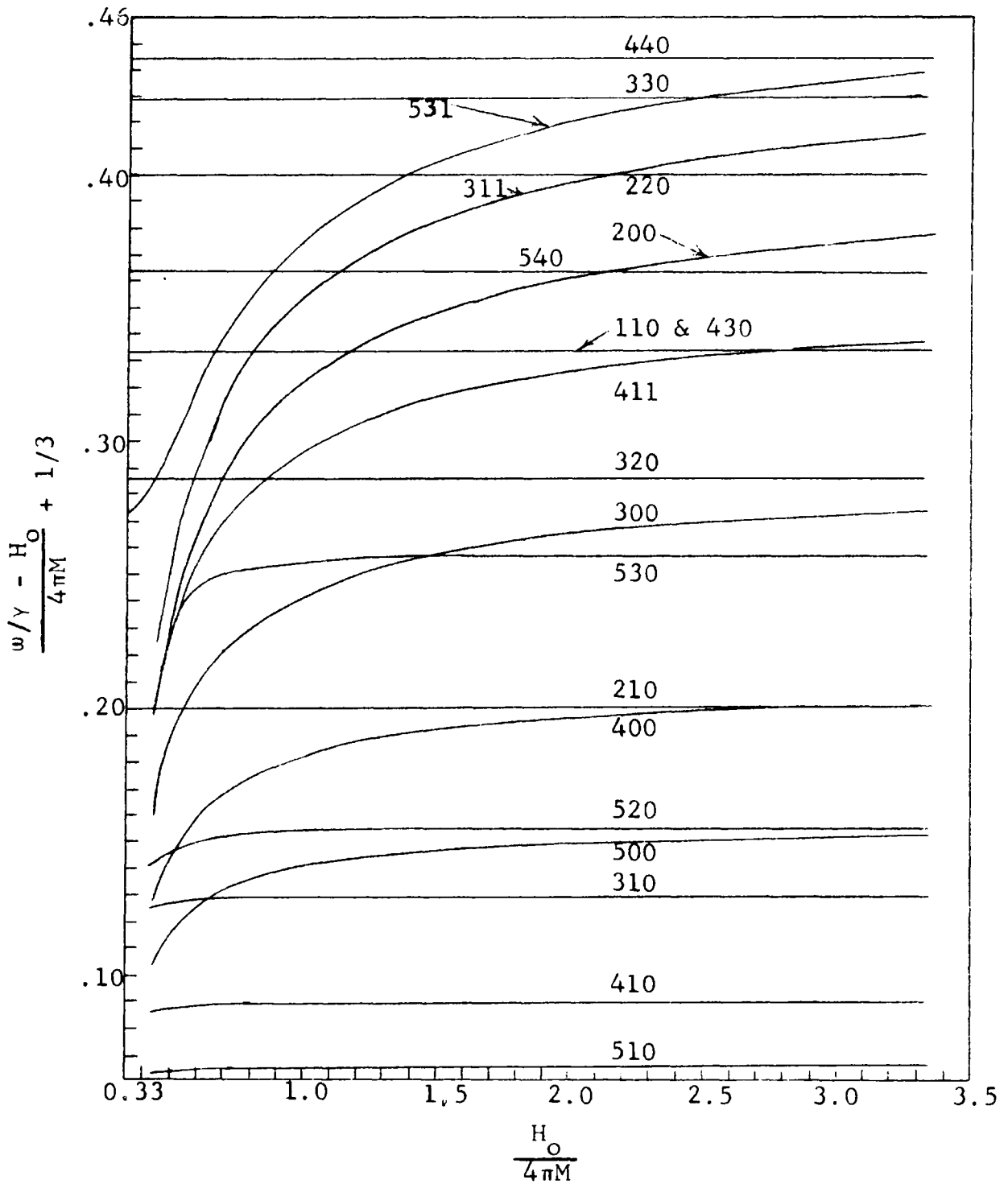


Figure 2.3.--Plot of  $(\omega/\gamma - H_0)/4\pi M_0$  Versus  $H_0/4\pi M_0 \gamma$  for Some of the Lower Order Walker Modes. (After Fletcher, Solt, and Bell, Physical Rev., vol. 114, No. 3, p. 740, 1959).

shift proportional to  $M_0$  towards the high field side and secondly, there is coupling between different modes where they are degenerate. This second effect broadens the line width and causes the two degenerate modes to shift apart. Because of the YIG's small magnetization this effect of coupling due to propagation is negligible, although coupling can also be caused by high power and surface irregularities.

Excitation of the Walker modes is dependent on the distribution of the rf magnetic fields within the ferrite media. The theoretical distribution within a sphere can be derived for each of the modes, but it is difficult to relate this to the fields that must exist external to the sphere for some of the higher order modes. If the field is uniform across the sphere, the dominant mode (1, 1, 0) will be excited. Similarly if the ferrite is placed in a field such that each half is driven directly out of phase the higher order mode (2, 1, 0) will be excited. It is also reasonable to assume that distortion of the fields by such discontinuities as irregular surface of the sample or the medium in which the sample is mounted would cause excitation of Walker modes.

#### 2.4 Theory of the Cross Guide Coupler

The cross guide coupler technique avoids the difficulties associated with high Q resonant cavities,

especially if the measurements are to be taken at various frequencies. A detailed analysis of the cross guide coupler as a means of measuring ferrite line widths may be found elsewhere,<sup>10</sup> but pertinent facts as they may apply to magnetostatic modes will be discussed herein. The discussion shall be limited to the coaxial coupler as opposed to the wave guide coupler, although the general theory applies equally well to both.

Physically, the test section consists of a machined brass block which has two holes drilled perpendicularly to each other through two adjacent faces as shown in Figure 2.4. These holes overlap slightly so that a small aperture is formed between the two. This aperture forms the coupling hole into which the ferrite is mounted. To the four openings in the brass block are connected four arms with center conductors that extend through the block. These arms provide the necessary connections to standard coaxial line.

An rf field of the desired frequency is introduced into one end of the primary arm while a short is adjusted in the other so as to produce an electric field null at the aperture. Since the magnetic field does not couple, no power is coupled into the secondary arm. The magnetostatic field is now applied normally to the broad face and adjusted for resonance. The tensor properties of the ferrite couple the transverse rf magnetic field in

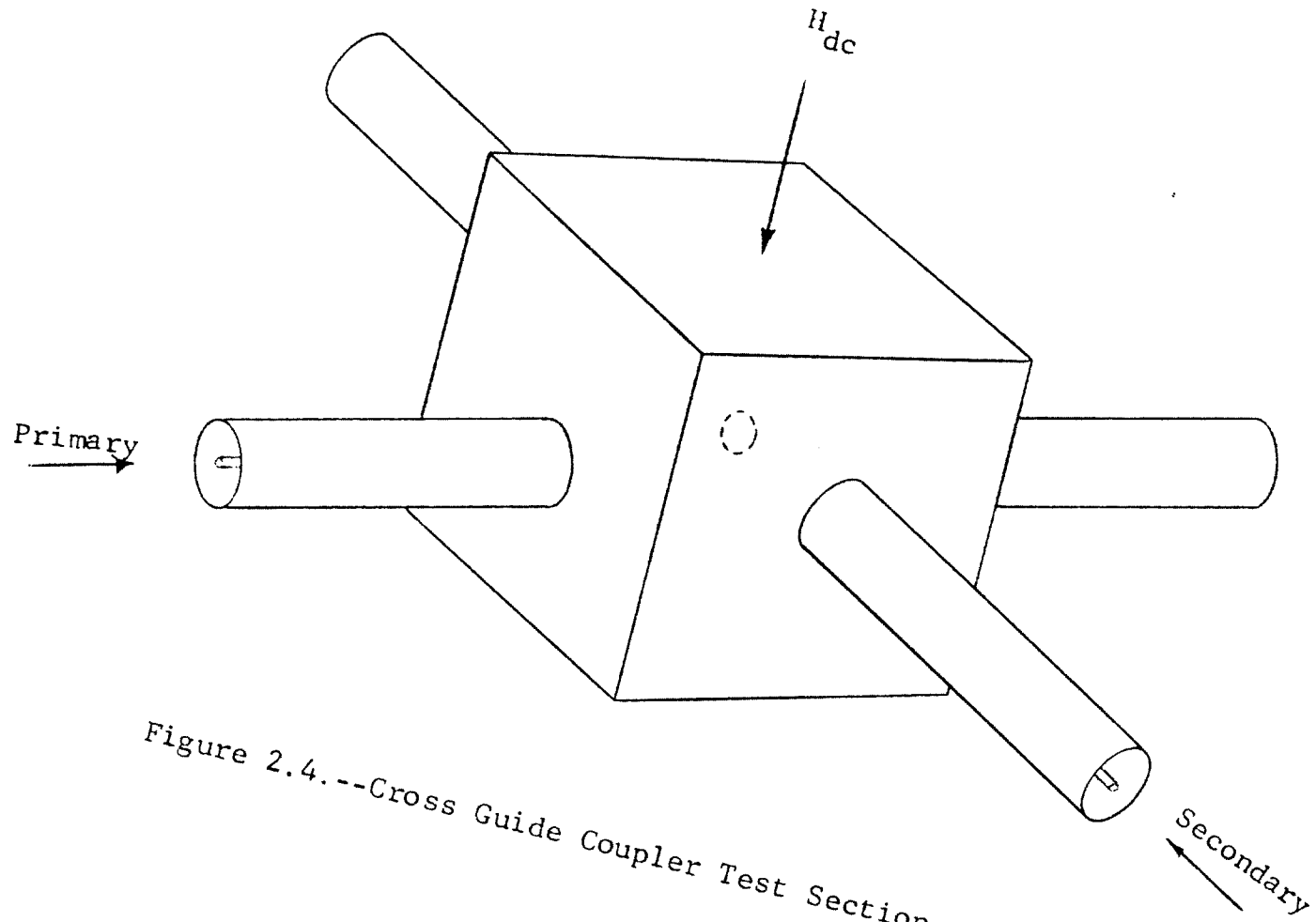


Figure 2.4.--Cross Guide Coupler Test Section.

a direction normal to the magnetostatic and the rf magnetic fields. This component is longitudinal in the primary arm and transverse in the secondary. Since the dominant mode of the coax is TEM power will be coupled to the secondary. It can be shown<sup>16</sup> that the magnetostatic field at the peak of the coupled power is identically the field observed at maximum absorption in a cavity.

Qualitatively this theory may be extended to include coupling of the Walker modes since the magnetostatic resonances are analogous to the uniform precessional mode, except that there is a variation in phase and amplitude of the rf magnetization in different zones within the ferrite itself.<sup>13</sup> Therefore, the tensor properties will induce a transverse rf magnetic field in the secondary arm in much the same manner as for the uniform mode. Thus the theoretical basis for exciting Walker modes in the cross guide coupler is established.

## CHAPTER III

### EXPERIMENTAL

#### 3.1 Experimental Arrangement

The physical arrangement of the components is indicated by the block diagram pictured in Figure 3.1.

The cross guide coupler test section was mounted between the pole faces of the magnet such that the magnetostatic field would be normal to the flat faces. A klystron and its associated power supply provided the microwave power within the coaxial line. This was monitored for frequency and power level by the frequency meter and the VSWR indicator in the primary. An adjustable short at the opposite end of the primary was adjusted so as to create a null of electric field at the aperture. The secondary consisted of a coaxial short circuit at one end and a detector tuned to the frequency of the primary at the other end. The detector was connected to another VSWR indicator to read power coupled from the primary to the secondary.

A precision gaussmeter consisting of a resonant probe and an integral oscilloscope indicated the strength of the magnetostatic field. To accurately determine the

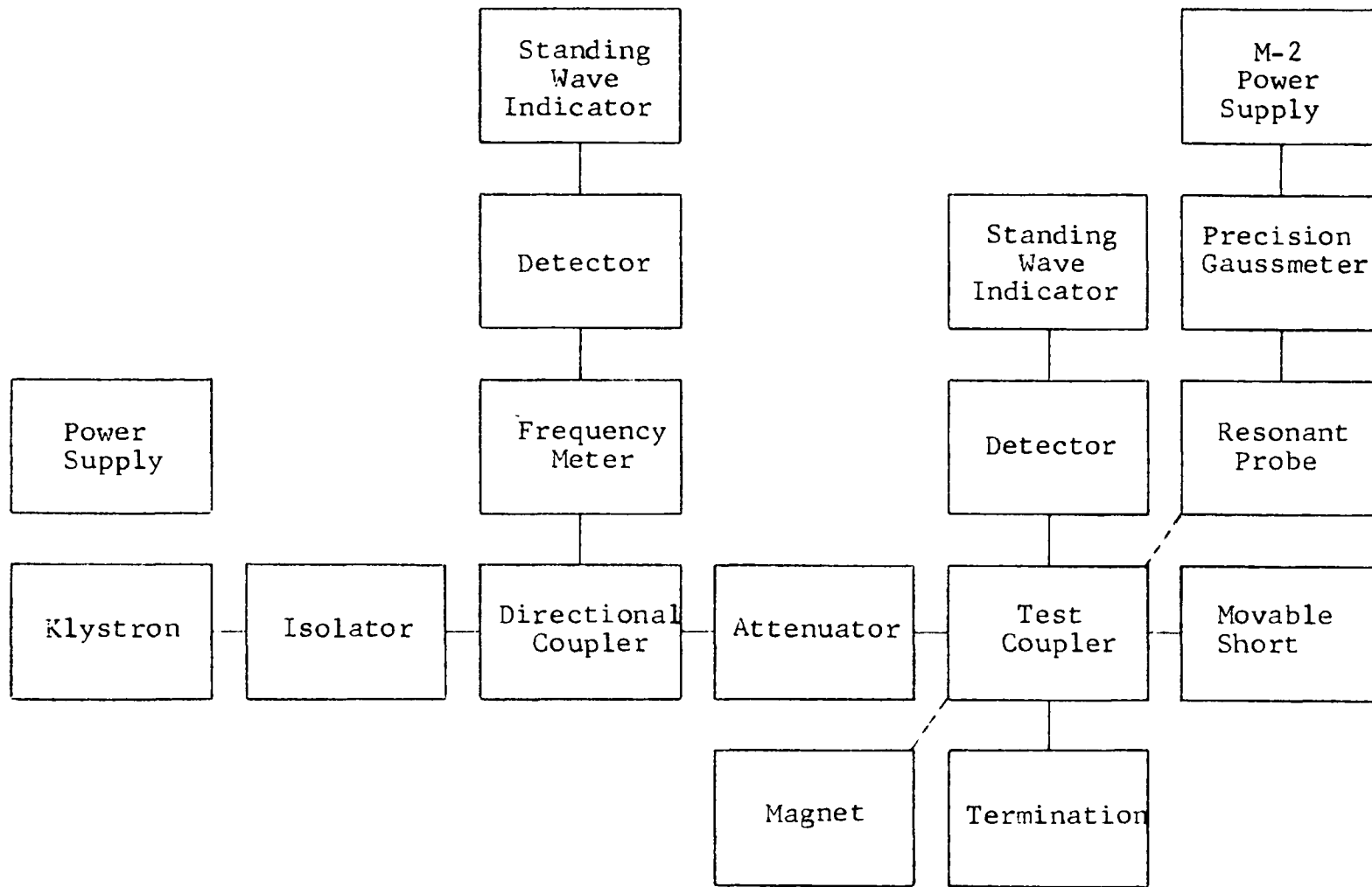


Figure 3.1.--Block Diagram of Component Arrangement.

probe resonance a signal generator was used to match frequency with the scope trace and this frequency was read on the electronic counter. The resonant frequency was subsequently converted to oersteds by means of tables supplied with the gaussmeter.

### 3.2 Sample Configuration and Mounting

The ferrite sample used throughout this experiment was a single crystal yttrium iron garnet previously used in line width measurements. The sample was very nearly spherical measuring 0.097 inches by 0.095 inches in diameter on its major and minor axes. The surface finish was that obtained by polishing on number 180 paper. This is a relatively coarse paper having grit sizes in excess of 70 microns. The surface of the sphere, when viewed through a 10 power microscope, appeared quite uniform except for a small triangular pit in one end. Due to the spherical shape it was decided that the sample, as described, would be used for the first half of the experiment without further preparation.

The aperture in the coupler test section had a diameter of 0.240 inches, or approximately two and one-half times greater than that of the sample. The ferrite sample was mounted at three different locations within the aperture to take advantage of the different rf field configurations

present. These three locations can best be visualized by referring to the cross section of the test coupler shown in Figure 3.2. Position one was with the sample centered in the aperture opening. In position two the sample was placed against the side of the aperture in the direction of the propagating rf field. For position three the YIG was again placed against the side of the aperture but ninety degrees from position two. The YIG sample was mounted in the aperture with Duco cement.

For the second half of the experiment, the surface of the YIG sphere was finely polished with 3/0 abrasive paper (approximate grit size 15 microns) and mounted again in the positions described in the preceding paragraph. The particular method used in polishing the sphere is explained elsewhere in the literature.<sup>17</sup> Suffice it to say that the sample was polished with successively finer grit paper until the desired finish was obtained. Although the surface finish was substantially improved, the small pit remained. The finer grit abrasives caused the sample to become out of round. This difficulty in producing perfect spheres is due to the anisotropy hardness<sup>18</sup> of the ferrite. The final sample size was 0.095 inches by 0.091 inches which was sufficiently spherical to allow for the neglect of axial ratio in computing the magneto-static field for the various modes.

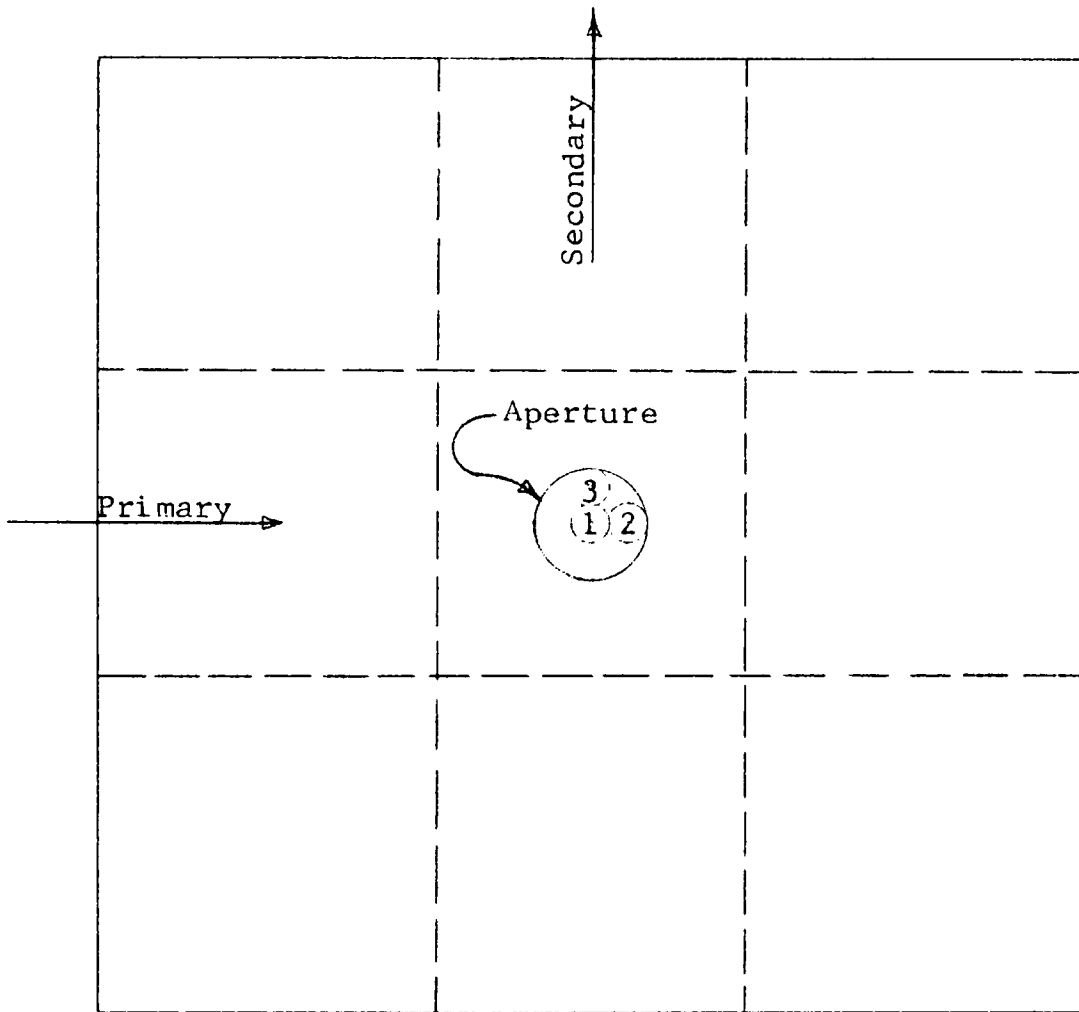


Figure 3.2.--Cross Section of Cross Guide Coupler Showing Locations of Ferrite Positions 1, 2, and 3 in the Aperture.

### 3.3 Measurement Procedure

For each position of the YIG in the aperture the general measurement procedure was the same. The klystron provided a discrete frequency between 0.9 and 4.5 gc. At each of these frequencies the magnetostatic field was slowly increased over the full range of the equipment. A plot was made of coupled power versus applied magnetostatic field paying particular attention to accurately measuring the magnetostatic field values for the resonant peaks and the 3db down points on the resonant curves. With this method not only could the modes be identified, but the line widths of each mode could also be determined. A similar plot was made at each of fifteen different microwave frequencies for each sample position. Due to the peculiarities of the equipment a particular rf frequency could not always be obtained so that an exact comparison could not be made between the different ferrite positions. In fact there was no single frequency common to all three ferrite positions for each of the two degrees of surface finish. This obvious disadvantage was overcome by the numerous frequencies chosen so that a general trend could be noted.

### 3.4 Characteristic Assumptions for the Sample

Due to the fact that certain specifications regarding the characteristics of the YIG sample were

unavailable, several assumptions had to be made. One of these assumptions was in regard to the "g" factor. The theoretical value for a single crystal YIG has been computed at a value of 2.00. This has been rigorously verified for x-band frequencies with a gradual increase to a value of 2.1 in the vicinity of 2 gc. For frequencies below 2 there is a marked increase. The "g" factor assumed in this experiment was 2.03 giving a value of 2.84 for  $\gamma$ .

The second assumption was for the value of  $4\pi M_0$ . For a single crystal YIG the magnetization is approximately 1750 gauss. Another method for determining the magnetization was advanced by Dillon.<sup>19</sup> Walker's theory predicts that (2, 1, 0) mode will occur  $(2/15)4\pi M_0$  above the (1, 1, 0) mode. Thus the spacing between these modes could be used as a microwave measure of the magnetization. Since the (2, 1, 0) mode, in addition to the uniform mode, appeared in all of the experimental plots for all sphere locations this method appeared to be superior to a simple assumption. The average spacing between these modes was 238 oersteds which predicts a value of 1786 gauss for the magnetization; therefore, 1786 gauss was used for all calculations instead of the assumed value of 1750.

The third assumption deals with the anisotropy field. Since no attempt was made to align the easy axis of the sphere with the magnetostatic field the anisotropy

field will have a twofold effect. First, there is an increase in resonant line width and secondly, the magnetostatic field will not correspond to  $\omega/\gamma$  when the easy axis is out of alignment with the magnetostatic field. The first effect is of no great concern since the line width broadening is affected more by other factors such as the pit in the end of the sphere than by the anisotropy. The second effect was accounted for by computing  $\omega/\gamma$  for each ferrite location and then applying a correction so that it corresponded to the magnetostatic field value for the dominant mode. This correction was applied equally to all values of dc applied field for that particular sample location. This amounts to a shifting of the H-axis a sufficient amount so as to make the magnetostatic field value of the dominant mode coincide with  $\omega/\gamma$ . This appears to be a reasonable assumption because the spacings of the various modes do not vary with the crystal direction along which  $H_{dc}$  is applied.<sup>18</sup>

### 3.5 Experimental Results

Six different plots of coupled power versus applied magnetostatic field are shown pictorially in Figure 3.3 and 3.4. These plots were for the three ferrite positions and the two degrees of polish. In each case the rf frequency was that which was closest to 3.75 gc.

70 micron polish

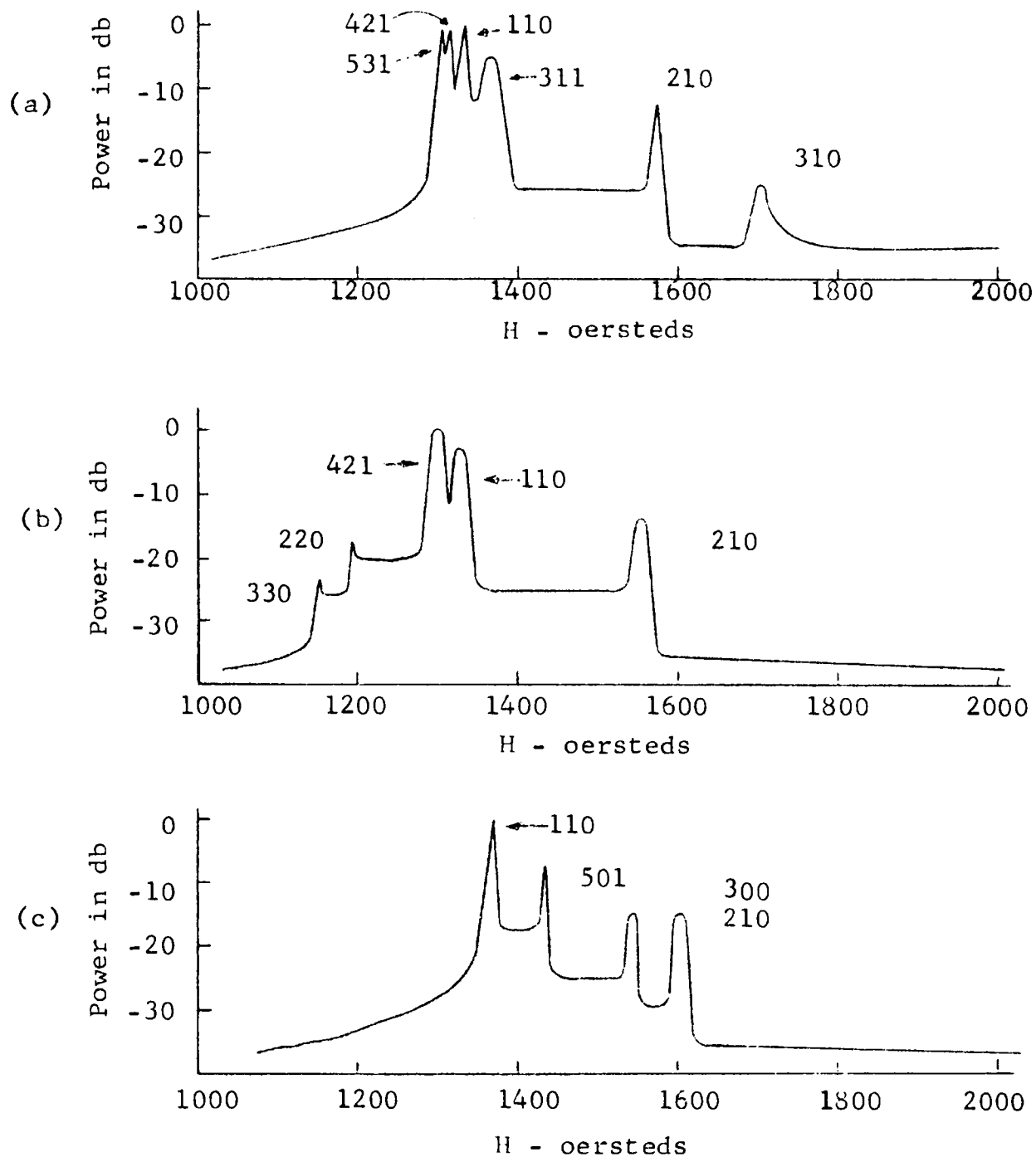


Figure 3.3.--Coupled Power Versus H Applied for 70 Micron Polished Ferrite. (a) Ferrite in position one at 3.79 Kmc, (b) ferrite in position two at 3.72 Kmc, (c) ferrite in position three at 3.75 Kmc.

## 15 micron polish

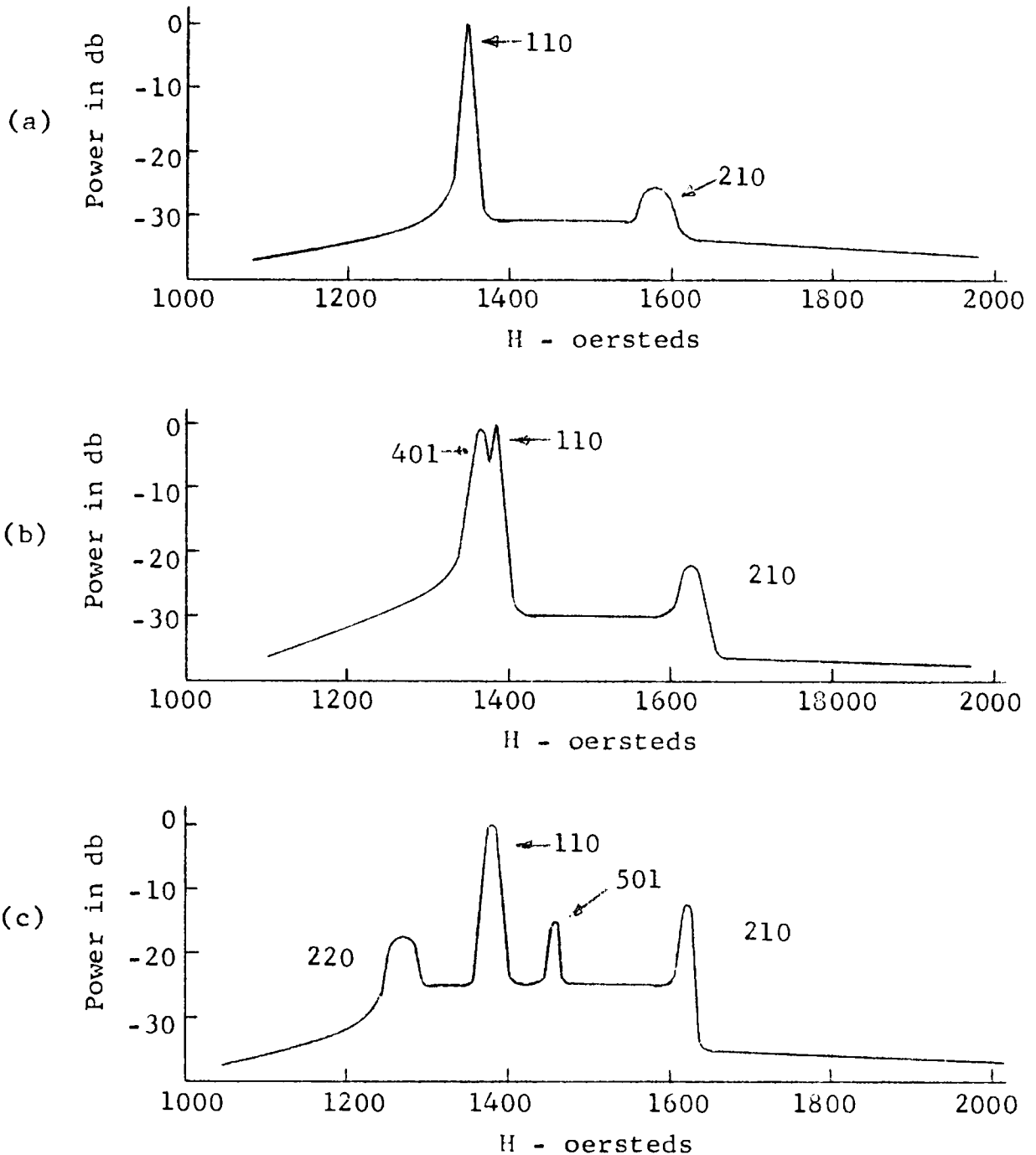


Figure 3.4.--Coupled Power Versus H Applied for 15 Micron Polished Ferrite. (a) Ferrite in position one at 3.75 Kmc, (b) ferrite in position two at 3.75 Kmc, (c) ferrite in position three at 3.75 Kmc.

With the exception of the (1, 1, 0) and the (2, 1, 0) modes (which were excited in every case) no conclusions could be drawn as to the effect of repositioning the ferrite within the aperture. The number of modes excited were a function of frequency rather than a function of position. As the frequency decreased the line width increased and the number of magnetostatic modes decreased. For frequencies below 1.7 gc the magnetostatic field necessary for resonance of the dominant mode is less than 600 gauss. Since this is less than  $4\pi M_0/3$  the YIG is not saturated and the dominant mode disappears. Similarly the (2, 1, 0) mode disappears below 1.05 gc. No resonant modes were observed below this frequency.

There was a decided decrease in the number of Walker modes that could be excited in the finely polished YIG with the exception of the polished sphere in position number three. In this configuration as many as six modes were excited at several different frequencies. The identification of the magnetostatic modes was performed in the following manner. For each rf frequency a line equal to  $\omega/\gamma 4\pi M_0$  showing the manner in which the modes are transversed as the magnetostatic field is varied was plotted on Figure 2.3. Figure 3.5 shows an example of this method for an rf frequency of 4.27 gc. The coupled

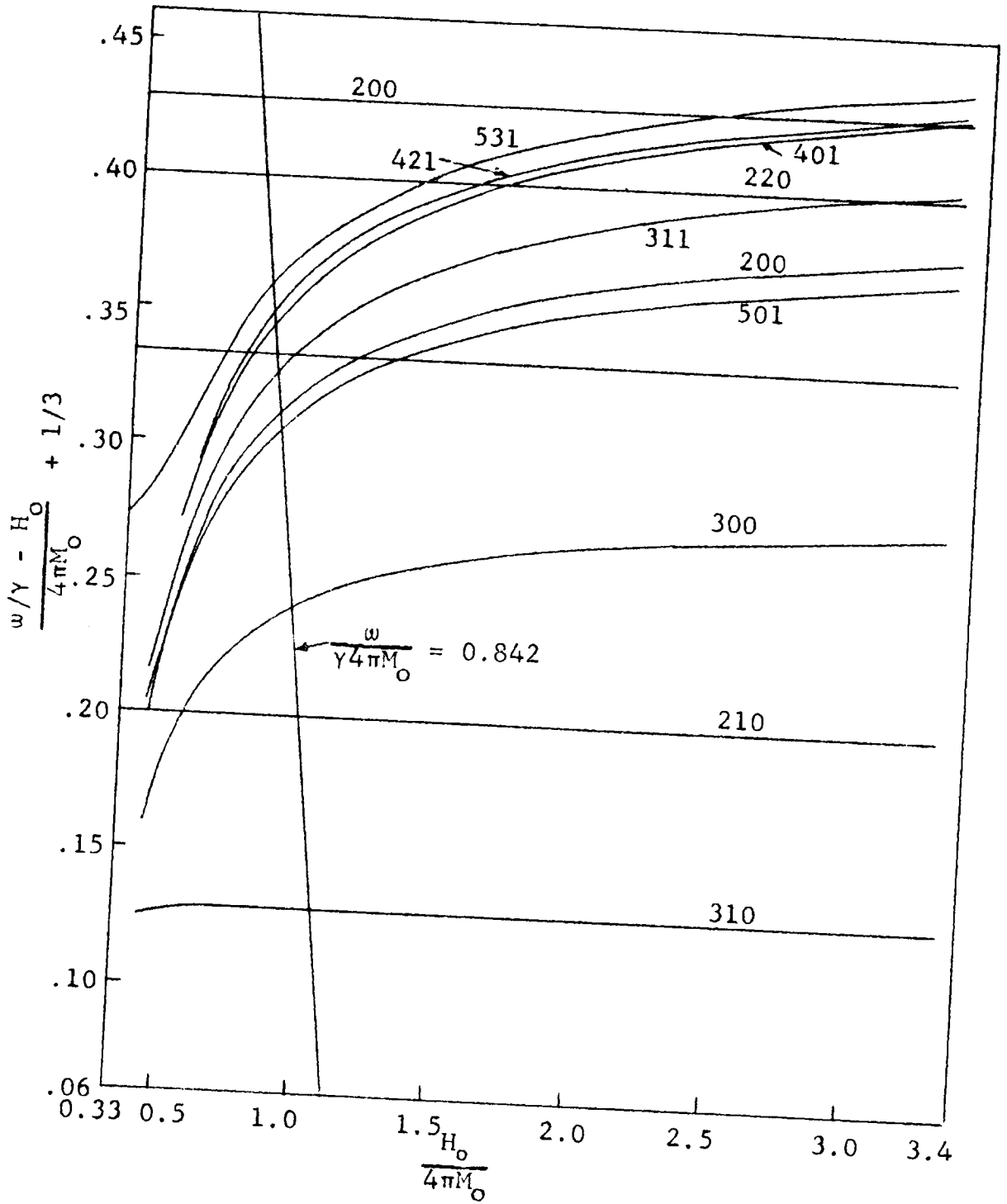


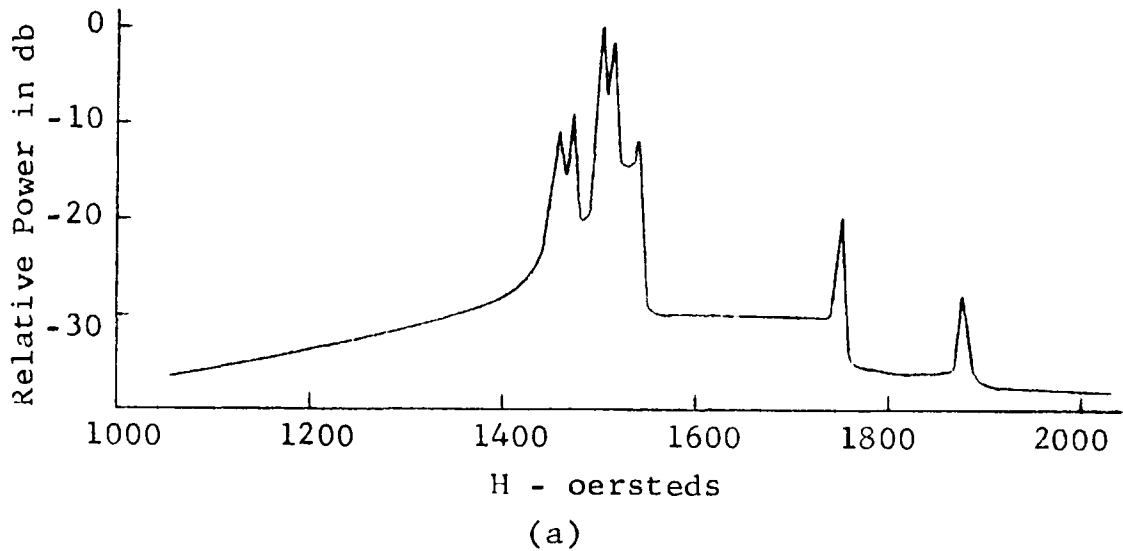
Figure 3.5.--Plot of  $\omega/\gamma 4\pi M = 0.842$  on Figure 2.3.

power versus the magnetostatic field is plotted in Figure 3.6a for the rough sphere centered in the aperture at this same rf frequency. The calculated values of H for a few of the simple modes and the corresponding observed values are tabulated in Figure 3.6b.

Although the particular modes that were excited could not be predicted in advance, they were readily identified using the cross guide coupler technique.

The line widths of the various modes ranged from 4 oersteds to about 35 oersteds for the completely saturated sample. The average line widths of the (1, 1, 0) modes for the 70 micron polished sphere were 7, 9, and 12 oersteds for sample locations 1, 2, and 3, respectively. Similarly, the line widths of the (2, 1, 0) modes were 7, 16, and 11 oersteds. This would seem to indicate that the line width of the (2, 1, 0) mode is approximately the same as that of the dominant mode which is in agreement with other observations.<sup>15</sup>

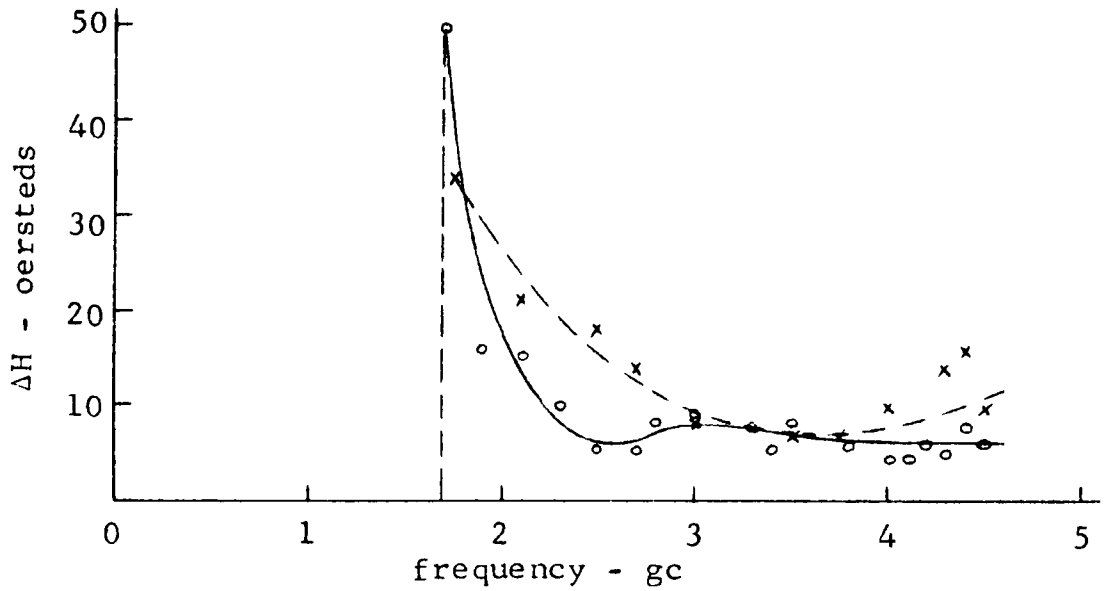
The frequency dependence of the line widths of the (1, 1, 0) mode are plotted in Figures 3.7, 3.8, and 3.9 for the sample locations 1, 2, and 3 respectively. The line width of the (1, 1, 0) mode is generally larger for the 15 micron polished sphere than for the 70 micron polish. This contradicts the fact that line width



Mode	$H_{calc}$	$H_{obs}$
330	1332	
220	1382	
531	1457	1460
401	1482	1473
311	1500	
110	1503	1502
311	1516	1516
200	1540	1540
411	1583	
300	1671	
210	1743	1752
400	1772	
310	1870	1873
410	1939	

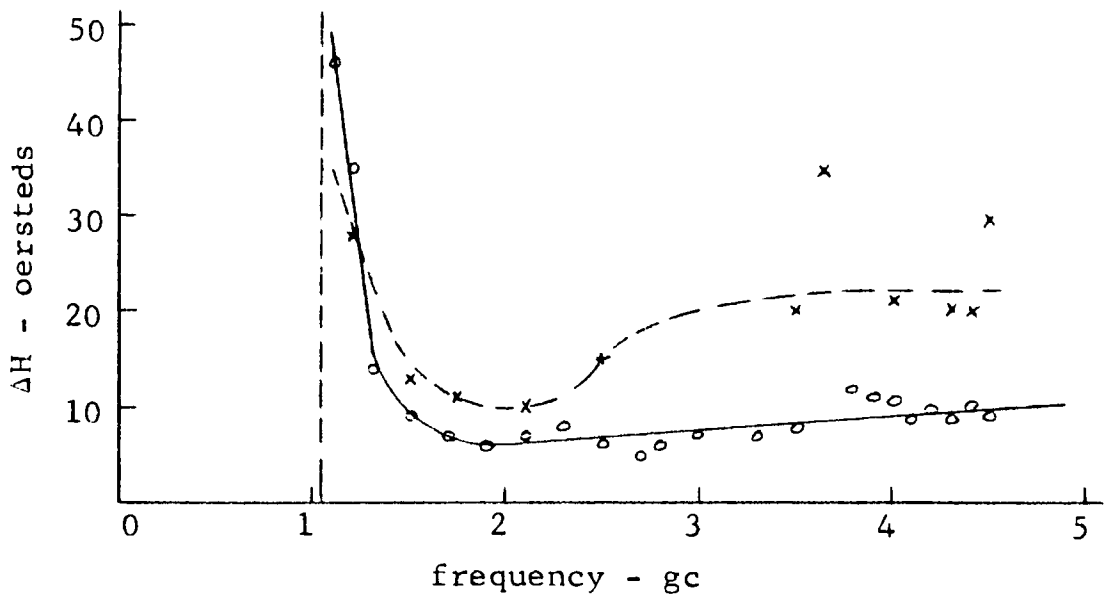
(b)

Figure 3.6.--Magnetostatic Modes in a Single Crystal YIG. (a) Coupled power versus H applied at 4.27 Kmc, (b) Table indicating calculated and observed values of H at 4.27 Kmc.



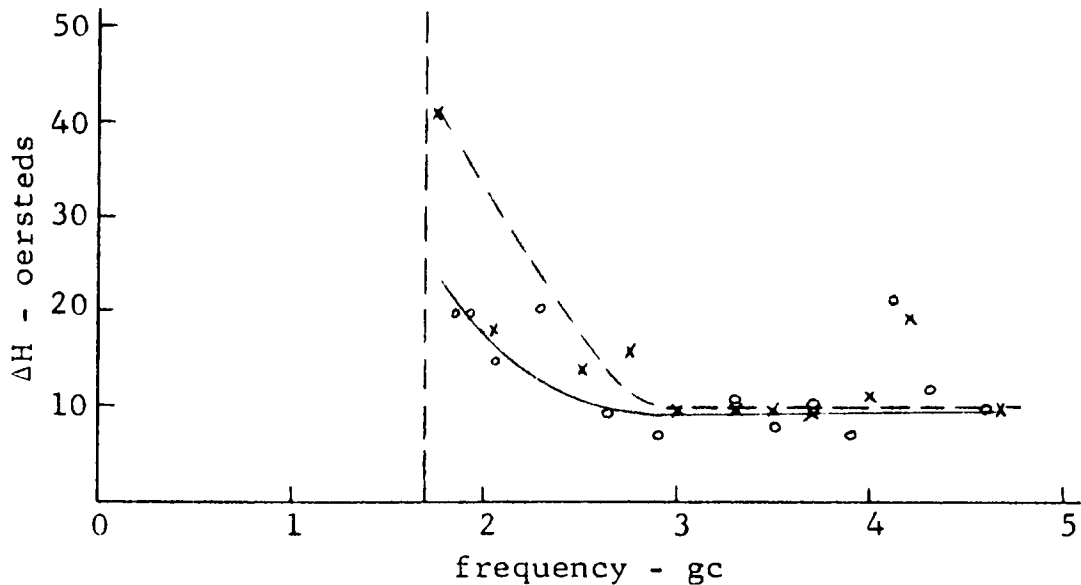
(a)

—○—○—○— 70 micron finish  
 —×—×—×— 15 micron finish

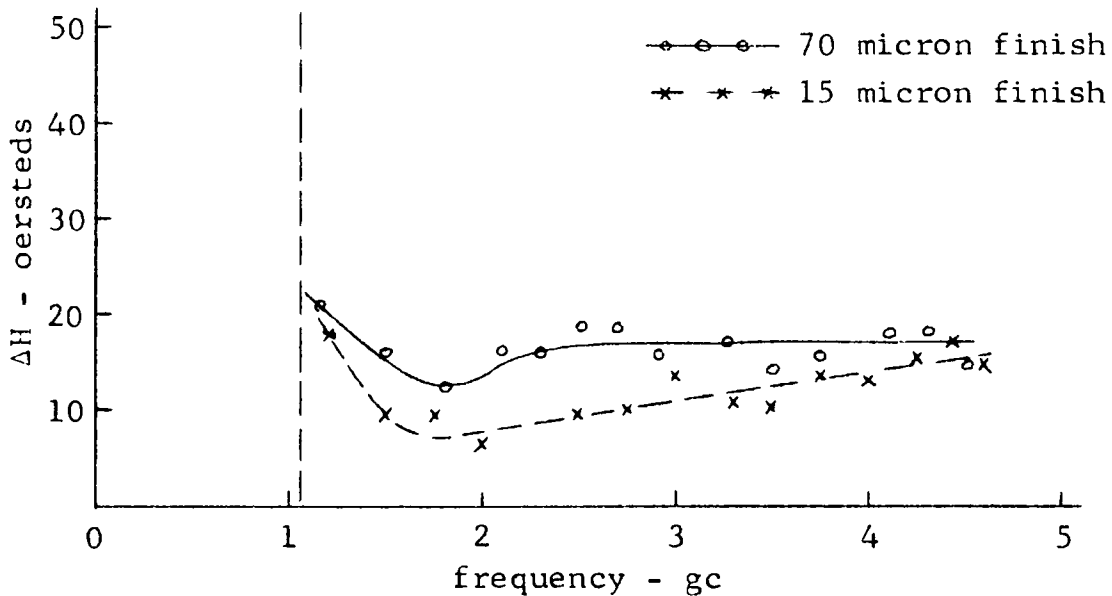


(b)

Figure 3.7.--Line Width as a Function of Frequency for the Sample in Position 1. (a) 110 mode, (b) 210 mode.



(a)



(b)

Figure 3.8.--Line Width as a Function of Frequency for the Sample in Position 2. (a) 110 mode, (b) 210 mode.

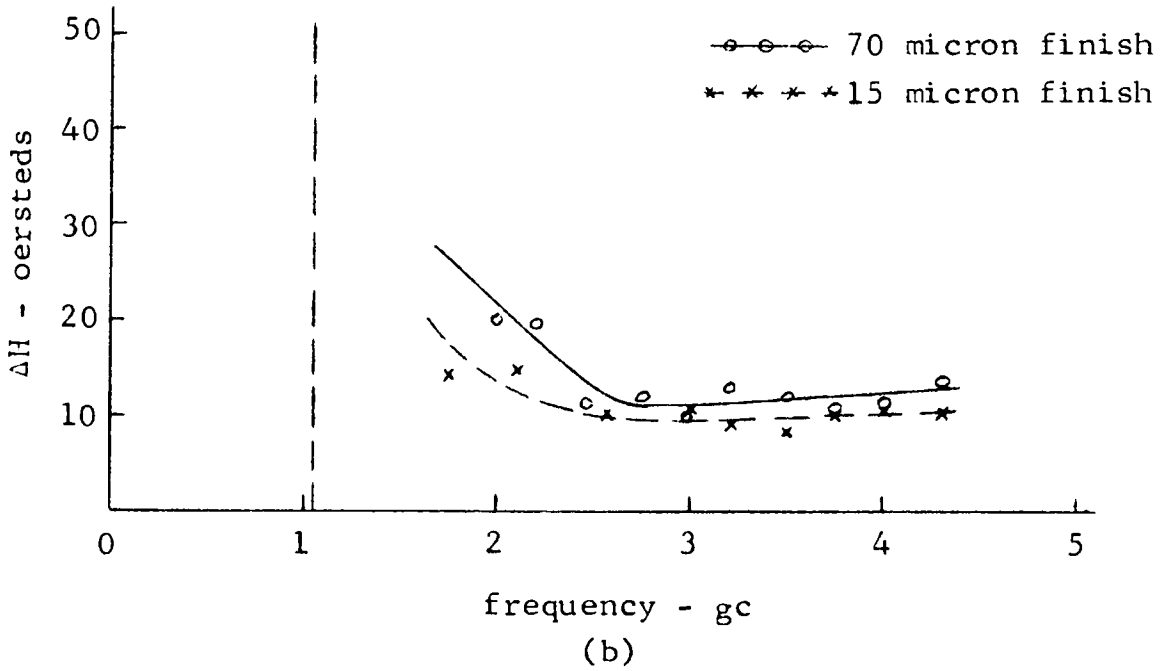
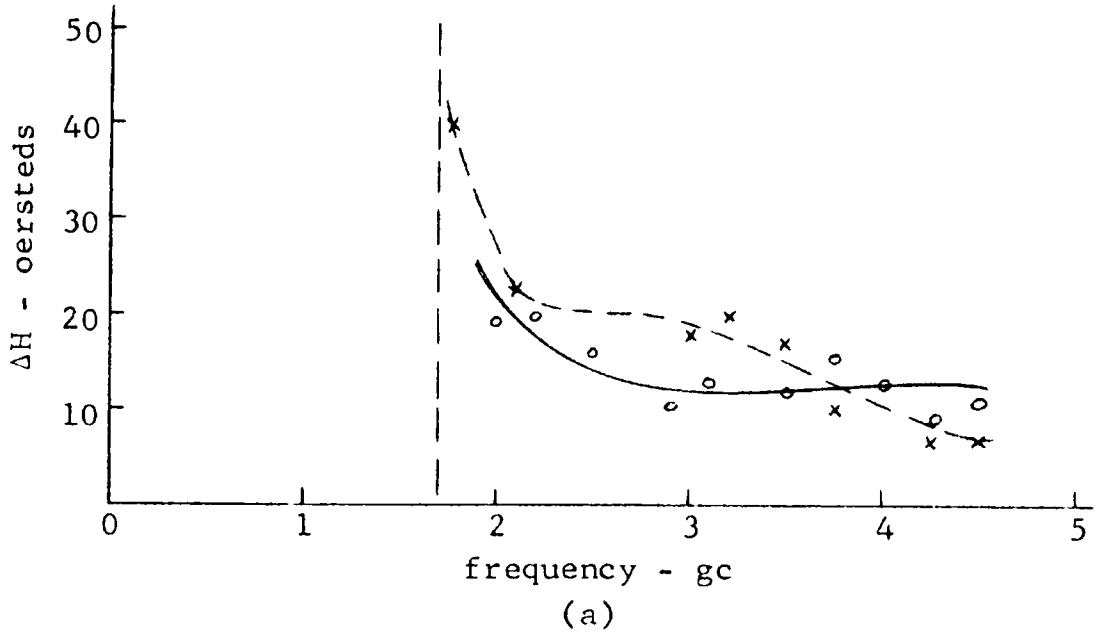


Figure 3.9.--Line Width as a Function of Frequency for the Sample in Position 3. (a) 110 mode, (b) 210 mode.

decreases as the surface finish is improved. Several factors could account for this discrepancy such as sample shape or non-uniform surface polish, but the author feels that the pit existing at the end of the sphere was the primary factor. As the surface of the sphere was improved the pit would appear as a larger discontinuity on the surface. This discontinuity would cause energy scattering from the uniform precession into degenerate spin waves, thus increasing the line width.

## CHAPTER IV

### CONCLUSIONS

#### 4.1 Conclusions

The following conclusions are based on the preceding theory and experimental results.

No definitive results were obtained as a consequence of repositioning the ferrite within the aperture. The particular Walker modes excited were different for each position but they did not follow a general trend. Each rf frequency excited a different set of modes when the ferrite was off center. This is probably due to the **non-uniform** rf fields within the sphere near the edge of the aperture.

Although the results were not entirely conclusive it appeared that the number of Walker modes excited in a cross guide coupler is dependent on the surface finish of the sphere. As the surface of the sample is improved the internal rf fields become more uniform with a corresponding decrease in the number of Walker modes excited.

The cross guide coupler technique is an effective means of exciting and identifying Walker modes. There is the distinct disadvantage that it does not seem possible

to predict in advance which modes will be excited, but this may possibly be overcome in the future by a more exacting orientation of the ferrite within the aperture.

It seems that the line widths of the different modes are essentially the same and that they behave similarly as a function of frequency.

#### 4.2 Recommendations for Further Study

A. Walker mode experiments should be extended into the x-band frequency range utilizing the cross guide coupler technique.

B. Further studies regarding the effect of sample shape and/or diameter on multiple ferrimagnetic resonance should be conducted.

C. The possibility of predicting the particular modes to be excited should be investigated more thoroughly.

## REFERENCES

1. J. L. Snoek, "Non-metallic magnetic material for high frequencies," Philips Tech. Rev., vol. 8, pp. 353-360; December, 1946.
2. H. Forestier and G. Guiot-Guillain, "A new series of ferromagnetic substances: the ferrites of the rare earth metals," Compt. Rend., vol. 230, pp. 1844-1850, 1950.
3. F. Bertaut and F. Forrat, "Structure of ferrimagnetic ferrites of rare earths," Compt. Rend., vol. 242, pp. 382-384, 1956.
4. J. W. Nielsen and E. F. Dearborn, "The growth of single crystals of magnetic garnets," J. Phys. Chem. Solids, vol. 5, p. 202, 1958.
5. R. L. White, I. H. Solt, and J. E. Mercereay, "Multiple ferromagnetic resonance absorption in manganese and manganese-zinc ferrite," Bull. Am. Phys. Soc., ser. 2, vol. 1, p. 12, 1956.
6. R. L. White and I. H. Solt, "Multiple ferromagnetic resonance in ferrite spheres," Phys. Rev., vol. 104, pp. 56-62, October, 1956.
7. J. F. Dillon, Jr., "Ferromagnetic resonance in thin discs of manganese ferrite," Bull. Am. Phys. Soc., ser. 2, vol. 1, p. 125, 1956.
8. L. R. Walker, "Magnetostatic modes in ferromagnetic resonance," Phys. Rev., vol. 105, p. 390-399, January, 1957.
9. P. Fletcher, I. H. Solt, Jr., and R. Bell, "Identification of the magnetostatic modes of ferromagnetic resonant spheres," Phys. Rev., vol. 114, No. 3, 739-745, May, 1959.
10. D. C. Stinson, "Ferrite line width measurements in a cross-guide coupler," IRE Trans., PGMTT-3, pp. 446-450; October, 1958.

11. C. L. Landry, "Line Width Behavior of Hybrid Single Crystal Garnet Ferrites," M. S. thesis, Dept. of Elec. Eng., University of Arizona, Tucson, Ariz.; May, 1962.
12. P. E. Tannenwald, "Spin waves," Microwave J., vol. 2, p. 25; 1959.
13. B. Lax and K. J. Button, "Microwave Ferrites and Ferromagnetics," McGraw-Hill Book Co., Inc., New York, N. Y.; 1962.
14. H. Suhl, "Origin and use of instabilities in ferromagnetic resonance," J. Appl. Phys., vol. 29, pp. 416-421; March, 1958.
15. L. R. Walker, "Resonant Modes of ferromagnetic spheroids," J. Appl. Phys., vol. 29, pp. 318-323; March, 1958.
16. D. C. Stinson, "Ferrite Line Width Measurements," University of Arizona, Paper No. CP 61-1005, pp. 1-8; August, 1961.
17. Ibid., p. 6.
18. J. F. Dillon, Jr., "Magnetostatic modes in ferromagnetic spheres," Phys. Rev., vol. 112, No. 1, pp. 59-63; October, 1958.
19. Ibid., p. 62.